The gleaner, the opportunist, and their common catcher: An ecological tale about coexistence

Lilla Zs. Kiss Toni Klauschies

Last update: October 27, 2025

Next steps (notes for & by Lilla)

- methods in text
- producing h-diagrams (or with other parameters)

1 Motivation

- Starting from the coexistence of species that share the same resource through relative nonlinearity, we want to study how this coexistence mechanism acts in extended food webs, such as an additional predator.
- Predation is also known to enable coexistence of multiple prey through different mechanisms: frequency-dependent predation by favoring the less abundant prey, growth–defense trade-off by introducing an additional limiting factor, possibly relative nonlinearity of predation by enabling the species to benefit (or suffer less) in different ways from variation in predation.
- We want to exclude multiple factors of predation and model a generalist predator without any frequency-dependent or -independent preference for the prey in our study. By doing so, we still introduce an emergent growth–defense trade-off, which is a fluctuation-independent coexistence mechanism in our model.
- We want to study the effects of relative nonlinearity on coexistence in this extended model, moreover, explore the effects of the interaction of relative nonlinearity and an emergent growth–defense trade-off.

2 Model description

The model consists of four interacting populations whose abundance is described by the following state variables: R for the autotroph resource, C_1 and C_2 for the two herbivorous consumers of the resource, and P for the generalist predator of C_1 and C_2. The resource growth is bottom-up limited by an environmental factor such as light or space (L).

We assume a linear uptake rate for the autotroph resource R and the generalist predator P, as well as no differences in the conversion efficiency between the two consumers ($e_C :=$ conversion efficiency of consumers C_1 and C_2). Then, the temporal changes of population dynamics are described by the following system of ordinary differential equations:

$$\frac{dR}{dt} = \left(a_R(L - R) - \sum_{i=1}^{2} \frac{a_i C_i}{1 + h_i a_i R} - d_R \right) R \tag{1}$$

$$\frac{dC_i}{dt} = \left(\frac{e_C a_i R}{1 + h_i a_i R} - a_P P - d_i \right) C_i \tag{2}$$

$$\frac{dP}{dt} = \left(e_P a_P (C_1 + C_2) - d_P \right) P \tag{3}$$

The system is fully parametrized by the following parameters: the attack rate of R, C_1, C_2 and P, denoted by a_R, a_1, a_2 and a_P, respectively; the handling time h_1 and h_2 of the consumers C_1 and C_2; the conversion efficiency of the consumers (e_C) and of the predator (e_P) and the constant mortality rates d_R, d_1, d_2, and d_P.

Non-dimensionalization

$\frac{dX}{dt} = \left[\frac{M}{VT}\right]$ (rate of density change)

$a_X = \left[\frac{V}{MT}\right]$ (attack rate: rate of encounter per unit of food density)

$X = \left[\frac{M}{V}\right]$ (density)

$h_X = [T]$ (handling time)

$d_X = \left[\frac{1}{T}\right]$ (death rate)

$e_X = [\ \ ]$ (conversion efficiency)

$$R' \coloneqq \frac{R}{L} \qquad C_i' \coloneqq \frac{C_i}{e_C L} \qquad P' \coloneqq \frac{P}{e_P e_C L}$$

$$t' \coloneqq t a_R L$$

$$a_i' \coloneqq \frac{e_C a_i}{a_R} \qquad a_P' \coloneqq \frac{e_P e_C a_P}{a_R} \qquad h_i' \coloneqq \frac{h_i a_R L}{e_C}$$

$$d_R' \coloneqq \frac{d_R}{a_R L} \qquad d_i' \coloneqq \frac{d_i}{a_R L} \qquad d_P' \coloneqq \frac{d_P}{a_R L}$$

$$\frac{dR'}{dt'} = \frac{1}{L a_R L}\left(a_R(L-R) - \sum_{i=1}^{2}\frac{a_i C_i}{1+h_i a_i R} - d_R\right) R \tag{4}$$

$$= R'\left(\left(1-\frac{R}{L}\right) - \sum_{i=1}^{2}\frac{\frac{a_i C_i}{a_R L}}{1+h_i a_i R} - \frac{d_R}{a_R L}\right) \tag{5}$$

$$= R'\left((1-R') - \sum_{i=1}^{2}\frac{a_i' C_i'}{1+h_i' a_i' R'} - d_R'\right) \tag{6}$$

$$\frac{dP'}{dt'} = \frac{1}{L e_P a_R L}\left(e_P a_P C_1 + e_P a_P C_2 - d_P\right) P \tag{7}$$

$$= P'\left(\frac{e_P a_P C_1}{a_R L} + \frac{e_P a_P C_2}{a_R L} - \frac{d_P}{a_R L}\right) \tag{8}$$

$$= P'\left(a_P' C_1' + a_P' C_2' - d_P'\right) \tag{9}$$

$$= P'\left(a_P'(C_1' + C_2') - d_P'\right) \tag{10}$$

$$\frac{dC_i'}{dt} = \frac{1}{e_C L a_R L}\left(\frac{e_C a_i R}{1+h_i a_i R} - \frac{a_P P}{1+h_P a_P (C_1+C_2)} - d_i\right) C_i \tag{11}$$

$$= C_i'\left(\frac{\frac{e_C a_i R}{a_R L}}{1+h_i a_i R} - \frac{\frac{a_P P}{a_R L}}{1+h_P a_P (C_1+C_2)} - \frac{d_i}{a_R L}\right) \tag{12}$$

$$= C_i'\left(\frac{a_i' R'}{1+h_i' a_i' R'} - \frac{a_P' P'}{1+h_P' a_P' e_C (C_1'+C_2')} - d_i'\right) \tag{13}$$

The equations consist only of non-dimensional parameters. Assuming a negligible basal mortality rate $d_R = 0$, they simplify to the following set of ordinary differential equations without the prime notation:

$$\frac{dR}{dt} = R\left((1-R) - \sum_{i=1}^{2}\frac{a_i C_i}{1+h_i a_i R}\right) \tag{14}$$

$$\frac{dC_i}{dt} = C_i\left(\frac{a_i R}{1+h_i a_i R} - a_P P - d_i\right) \quad (i = 1,\ 2) \tag{15}$$

$$\frac{dP}{dt} = P\left(a_P(C_1+C_2) - d_P\right) \tag{16}$$

In the baseline model (see also Fig. 1) with relative nonlinearity between the consumers C_1 and C_2, one consumer is assumed to exhibit a linear functional response ($h_1 = 0$) and the other a saturating type II functional response ($h_2 > 0$):

$$\frac{dR}{dt} = R\left((1-R) - a_1C_1 - \frac{a_2C_2}{1+h_2a_2R}\right) \tag{17}$$

$$\frac{dC_1}{dt} = C_1\left(a_1R - a_PP - d_1\right) \tag{18}$$

$$\frac{dC_2}{dt} = C_2\left(\frac{a_2R}{1+h_2a_2R} - a_PP - d_2\right) \tag{19}$$

$$\frac{dP}{dt} = P\left(a_P(C_1+C_2) - d_P\right) \tag{20}$$

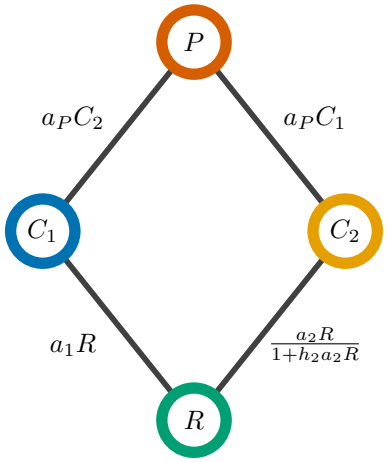

Figure 1: Visual representation of the feeding interactions of the baseline model (with relative nonlinearity of the consumers and generalist predation)

3 Methods

- coexistence checked either through numerical simulation or mutual invasion (depending on the functional response types)
- mortality rate plane (DONE)
- constructing models for comparison (DONE)
- FFT? (not used in the final version)
- intermittency index? (cite)

3.1 Construction of comparable models without (strong) relative nonlinearity

As we intend to assess both the individual and joint effects of relative nonlinearity and generalist predation, we constructed models that exhibit either no relative nonlinearity (with only linear functional responses), weak relative nonlinearity (with saturating functional responses but without supporting coexistence on its own) and with strong relative nonlinearity (the baseline model with linear and saturating functional responses), both with and without predation. As a result, we expect to see individual effects of predation and relative nonlinearity on the coexistence of competitors, as well as evaluate the interaction of the two coexistence mechanisms. The models with no or weak relative nonlinearity are described below, whereas the model with relative nonlinearity is the baseline model described in Section 2. When excluding predation, the same models are used with an initial predator density of $P = 0$.

3.1.1 Models without relative nonlinearity (aka Linearizing the saturating response, coexistence only based on the emergent growth–defense trade-off)

By the following method, we obtain a comparison model without relative nonlinearity by linearization of the saturating response of C_2. The functional response of C_1 remains linear, yielding a model with only linear functional responses for C_1, C_2 and P.

For a consumer with saturating functional response and per-capita net growth rate $f(R) = \frac{a_2 R}{1+a_2 h_2 R} - d_2$ with attack rate a_2, handling time h_2 and mortality rate d_2, the attack rate of the linearized functional response is defined as $a_L := a_2 \cdot (1 - d_2 h_2)$, and the mortality rate as $d_L = d_2$. By this definition, the minimal resource requirement and the mortality rate of C_2 remain the same, which are important parameters of the model and enable the direct comparison of the coexistence areas on the mortality rate plane. Figure 2 shows an example of a saturating functional response with the respective linearized functional response.

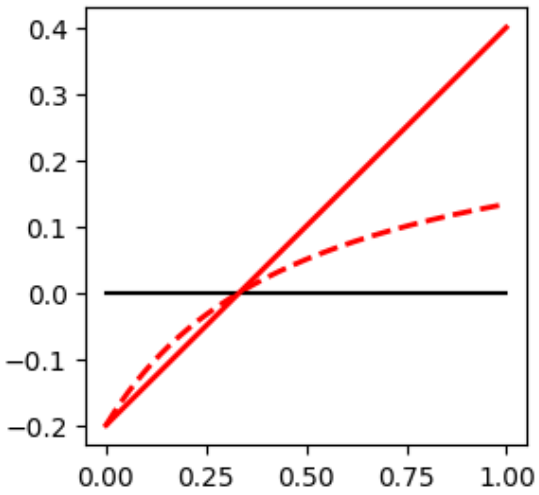

Figure 2: Example of the linearization of a saturating functional response

3.1.2 Models with weak relative nonlinearity

As the combined model shows similar intermittent dynamics in some parameter regions to the model with only relative nonlinearity, we asked the question: can the intermittent dynamics also be present without strong relative nonlinearity or is this a characteristic of relative nonlinearity in this model? Since the previous model with strictly linear functional responses does not allow stable limit cycle dynamics, we construct a model with saturating functional responses that only exhibit weak relative nonlinearity (hopefully, let's see later). Culprits: (1) we cannot get rid of relative nonlinearity entirely (2) we have to see if this model allows limit cycles in the parameter regions we are interested in, the curvature might not be enough.

In the strict sense, relative linearity is present when the difference of the functional responses is a linear function: $f_A(R) - f_B(R) = \frac{a_A R}{1+a_A h_A R} - \frac{a_B R}{1+a_B h_B R} = cR$ for a $c \in \mathbb{R}$ and $\forall R \in [0, 1]$. However, two different saturating functional responses cannot fulfill this criterion. Our consequent approach is to define a saturating functional response that exhibits only low relative nonlinearity to another saturating response. The following method produces a saturating per-capita growth rate with parameters a_S, h_S and d_S (based on a linear per-capita growth rate with parameters a_1 and d_1) which only exhibits a low relative nonlinearity to the saturating response given by a_2 and h_2 by fulfilling the criterion $\frac{f_S(R)}{f_2(R)} = \frac{\frac{a_S R}{1+a_S h_S R}}{\frac{a_2 R}{1+a_2 h_2 R}} = c$ for a $c \in \mathbb{R}$ and $\forall R \in [0, 1]$. The definition is met by the following parameters:

$$c = \frac{a_1}{a_2} + h_2 \cdot d_1 \tag{21}$$

$$a_S = c \cdot a_2 \tag{22}$$

$$h_S = \frac{h_2}{c} \tag{23}$$

$$d_S = d_1. \tag{24}$$

Additionally, the per-capita net growth rate $\frac{a_S R}{1+a_S h_S R} - d_S$ leads to the same minimum resource requirement as the linear per-capita net growth rate $a_1 R - d_1$, since $R^* = \frac{d1}{a1}$ in both cases.

In the model analysis with two saturating responses that only exhibit a low relative nonlinearity, coexistence was not observed. This suggests that relative nonlinearity was sufficiently low.

Measuring relative nonlinearity quantitatively? https://www.zoology.ubc.ca/bdg/pdfs_bdg/2013/fall/chesson/Chesson_2008.pdf

3.2 Establishing the coexistence likelihood in different models

In order to study the coexistence in the extended food web and the effect of predation on the coexistence, we quantify the likelihood for the stable coexistence of all species (including the predator when present in the model). Following [**?**], we use the proportion of parameter sets that allow for coexistence as a proxy to quantify the coexistence likelihood in the different models. The quantification is based on the parameters of the two consumers C_1 and C_2 that are present in all models. Of these, the attack rates and handling time(s) are not strictly bounded from above. When the mortality rate exceeds a threshold, the population cannot persist on the resource even without competition, making it impossible for the population to coexist in the complete model. Thus, there is a maximum mortality rate which is meaningful to consider for the quantification of coexistence likelihood. This is defined by a positive growth when the resource R is at its carrying capacity R_R^* and in the absence of any competition, $d_i^{\max} = \frac{a_i R_R^*}{1+a_i h_i R_R^*}$. The carrying capacity or equilibrium density of the resource in the system without consumers can be inferred from Eq. 14 (with $C_1 = C_2 = 0$) and is $R_R^* = 1$. Hence, $d_i^{\max} = \frac{a_i}{1+a_i h_i}$. The maximum mortality rates for C_1 and C_2 define a bounded parameter region $d_1 \times d_2$. For given attack rate and handling time parameters, as well as for given parameters of the predator (when relevant), the proxy for the coexistence likelihood can be calculated by quantifying the area on the $d_1 \times d_2$ parameter plane that allows coexistence of all populations in the system. The proportion of (d_1, d_2) pairs supporting coexistence is approximated numerically by dividing the parameter region into a 100×100 grid (with equal distances between grid points). For all grid points, the outcome of the population dynamics (long-term coexistence or exclusion of one or more population) is assessed and the proportion of grid points that allow coexistence gives the relative size of the coexistence area (relative to the $d_1 \times d_2$ region). The absolute size of the coexistence area is the relative size multiplied by the size of the feasible parameter region $d_1 \times d_2$.

When the model assumptions allowed, we used analytical criteria to assess the outcome of population dynamics (such as coexistence or exclusion) in the models.

In the model with only linear functional responses (both for the consumers and the predator), the four-species point equilibrium is stable. We scored a grid point on the $d_1 \times d_2$ parameter plane as supporting when the point equilibrium is positive for all species.

In the models without predation, we used the mutual invasion criteria as coexistence criteria, i.e., the criteria that both consumers exhibit a positive growth rate when their density is negligibly small and the population density of the resource and the other ('resident') consumer is at their (constant or dynamic) equilibrium. In case the resident population C_i exhibits a linear functional response, the stable long-term equilibrium density of the resource $R_{R-C_i}^*$ can be computed directly from Eq. 15 (with $h_i = 0$ for a linear functional response): $R_{R-C_i}^* = \frac{d_i}{a_i}$. Then, the consumer absent from the system (C_j) can invade if its growth rate at this resource density is positive, i.e., if $\frac{a_j R_{R-C_i}^*}{1+a_j h_j R_{R-C_i}^*} \geq 0$. In case the resident population exhibits a saturating functional response, the stability of the fixed-point equilibrium $R_{R-C_i}^*$ is not guaranteed and limit cycle behavior can occur. For that reason, we numerically simulate the population dynamics of the $R - C_i$ subsystem for 100 000 time steps (starting from an initial density of 0.01 for both the resource and the resident consumer), approximating the average invasion rate $\int \frac{a_j R(t)}{1+a_j h_j R(t)} dt$ (≥ 0) over the last 10 000 time steps. In case both species have a positive growth rate when negligibly rare, the coexistence of C_1 and C_2 on R is protected from the exclusion of both species.

In the models where the predator population P is present (except for the solely linear model described previously), we assessed coexistence based on the numerical simulation of the whole system at each grid point on the $d_1 \times d_2$ parameter region as the mutual invasion criteria for each species is increasing in restrictiveness. By conducting numerical simulations of the whole system, locally but not globally stable coexistence states may also be assessed that would not be covered by the mutual invasibility criteria. We simulated the population dynamics for 100 000 steps and evaluated the last 10 000 time steps for coexistence. The dynamics where regarded as showing long-term coexistence when all populations had an average density greater than 10^{-10} over the

evaluated time interval. Moreover, we assessed the type of equilibrium (fixed point or oscillatory equilibrium) numerically by computing the coefficient of variation and scoring the coexistence as oscillatory when it exceeded 0.01. The individual simulations were run in continuation, starting from the middle of the 100×100 grid and continuing in a (right-hand) spiral pattern outwards. The initial conditions of the population densities were set equal to the last population densities of the previous run and increased by 10^{-4} to support the invasion of all populations. The initial densities for the first simulation were set to 0.01 for all species.

4 Results

4.1 Interior equilibrium point of the four-species system

From Eqs. 18 and 19, the equilibrium abundance of the predator can be calculated in two ways:

$$\frac{a_1 R^* - d_1}{a_P} = P^* = \frac{\frac{a_2 R^*}{1+h_2 a_2 R^*} - d_2}{a_P} \tag{25}$$

The two equal expressions provide an equation for the equilibrium resource abundance.

After multiplication by a_P:

$$a_1 R^* - d_1 = \frac{a_2 R^*}{1 + h_2 a_2 R^*} - d_2 \tag{26}$$

$$| \cdot (1 + h_2 a_2 R^*)$$

$$a_1 R^* \cdot (1 + h_2 a_2 R^*) - d_1 \cdot (1 + h_2 a_2 R^*) = a_2 R^* - d_2 \cdot (1 + h_2 a_2 R^*) \tag{27}$$

$$a_1 h_2 a_2 {R^*}^2 + (a_1 - d_1 h_2 a_2) R^* - d_1 = (a_2 - d_2 h_2 a_2) R^* - d_2 \tag{28}$$

$$| - (a_2 - d_2 h_2 a_2) R^* + d_2$$

$$a_1 h_2 a_2 {R^*}^2 + \big(a_1 - a_2 - (d_1 - d_2) h_2 a_2\big) R^* - (d_1 - d_2) = 0 \tag{29}$$

The equation is quadratic for R^* and can be solved using e.g. the quadratic formula. Note that R^* does not depend on the parameters of P.

There are up to two interior equilibrium points, denoted by E_+ and E_-, where E_+ stands for the solution with "+" in the quadratic formula, and E_- corresponds to the solution with "−". We have a script for checking whether they are positive and locally stable (but this has not been systematically analyzed).

Note that cycles can appear with our without a positive unstable equilibrium point in the 4-species system.

4.2 Coexistence area on the parameter plane

We found that the effect of including a predator in the system strongly depends on the functional responses of the two prey species C_1 and C_2. We identified four main scenarios that are representative of the possible outcomes (see Fig. 3).

In the first case (Fig. 3a), the saturation of the functional response of C_2 is very slow (due to a low handling time h_2) and cannot produce the oscillations that are necessary for the coexistence of C_1 and C_2 without the predator. Yet, in the presence of the predator, the two consumers can coexist at a stable fixed-point equilibrium, in this case at the stable E_- equilibrium point. The coexistence area (red shading) is delimited from above by the invasion boundary of C_1 in the $R{-}C_2{-}P$ system (dashed red line) and from below by the invasion boundary of C_2 in the $R{-}C_1{-}P$ system (solid red line) and the boundary along which the two consumers exhibit an equal minimal resource requirement (solid black line). Since the coexistence is not enabled through fluctuations of the resource abundance, the coexistence mechanism at play is not the relative nonlinearity of competition between C_1 and C_2 but a fluctuation-independent, emergent growth–defense trade-off. More about the emergent trade-off here or somewhere else? The additional predation can thus enable coexistence when it is not possible without it.

In the second case (Fig. 3b), the saturating functional response is moderately curved (due to increasing handling time) and produces consumer–resource oscillations below the Hopf bifurcation point (... line). The resource fluctuations enable coexistence in the baseline model without the predator through the relative nonlinearity of competition between C_1 and C_2 in the gray-shaded area. However, when introducing the predator in this region of coexistence, it invades the system

and leads to one of the consumers being outcompeted. We also find no coexistence at a fixed-point equilibrium as in the previous case (due to the equilibrium points being unstable). Thus, this scenario shows that the addition of predation can have detrimental effects on the coexistence, destroying the coexistence that was possible without a predator. The model including predation shows bistability (priority effect) in the area below the invasion boundary of C_1 (where C_1 cannot invade the $R - C_2 - P$ system) and above the invasion boundary of C_2 (where C_2 cannot invade the $R - C_1 - P$ system), as both the $R - C_1 - P$ and the $R - C_2 - P$ systems are locally stable.

In the third case (Fig. 3c), the functional response of C_2 is moderately curved, due to a higher attack rate while keeping the handling time relatively low. The baseline model enables coexistence via relative nonlinearity of competition in the gray-shaded region. With the inclusion of the predator, the coexistence region shifts and extends above the invasion boundary of C_2 (solid black line) and consists of two areas: in the red-shaded are, the coexistence of the four species occurs at a dynamic equilibrium, whereas in the narrow region indicated by yellow, the coexistence is at the locally stable fixed-point equilibrium E_-. The coexistence regions with and without the predator strongly overlap, but the coexistence region with the predator is larger. The oscillatory dynamics and the overlap with the baseline coexistence area suggest that relative nonlinearity of competition between C_1 and C_2 is still an active coexistence mechanism (in certain parts of the parameter region) even when the predator is included. We also observe bistability in this model: the coexistence state in the area above the invasion boundary of C_2 in the $R - C_1 - P$ system (solid red line) is only locally, not globally stable.

[Due to the change in the attack rate and handling time (something more specific with a_P and d_P?), the predator cannot invade the $R - C_2$ subsystem or persist on C_2 alone. Hence, the invasion boundary of C_1 in the $R - C_2 - P$ system is also missing.]

In the fourth case (Fig. 3d), the saturation in the functional response of C_2 happens very rapidly (due to a very long handling time h_2), which leads to consumer–resource fluctuations in a large part of the parameter plane and a large coexistence region in the baseline model without predation. With the addition of the predator, we observe a similar emergent growth–defense trade-off as in the first case (cf. Fig. 3a) between the invasion boundaries of C_1 and C_2 in the system with the other consumer and the predator. In this case, the equilibrium point coincides with the E_+ equilibrium point. Coexistence outside this area is not possible in the 4-species model, as the invasion of the predator leads to the extinction of one of the consumers. The similarity between the first and fourth cases might be explained by the fact that the saturating response is so quickly saturating that —once saturation is reached— the functional response is nearly linear on a large interval of the resource density, leading to a similar outcome as the nearly linear functional response in the first case. Overall, the predation shifts the coexistence area to a different region of the parameter space and enables coexistence in a similarly large area through the emergent growth–defense trade-off.

4.3 Types of coexistence area [earlier notes]

The coexistence of all four species is possible at a stable equilibrium point (which is enabled by the predator/by the fluctuation-independent growth–defense trade-off only) or along a stable limit cycle (might be chaotic or quasi-periodic?). In the latter case, the interplay between the coexistence mechanisms is not clear. (To which degree does each mechanism contribute to an oscillatory coexistence?)

If the coexistence area is extended outside the invasion boundary of C_1 in the $C_2 - R$ system, the coexistence in these areas tends to show higher intermittency (consistent with the intermittency being higher near the boundary in the original model). Thus, we seek a way to differentiate between the intermittent cycles dominated by the gleaner–opportunist trade-off and those by the growth–defense trade-off.

4.4 Bifurcation diagrams for 3c

4.5 Bistability, multistability

The system shows bistability (or even multistability) in some parameter regions. This makes the analysis of the system more complicated since the outcome depends on the initial conditions. (See next paragraph.) Exploring the whole phase space over a parameter region is not feasible. An example of two locally stable limit cycles with different dynamical pattern is shown in Fig. 6. The purple limit cycle's basin of attraction seems smaller and is harder to find, whereas the yellow path is more stable/resilient against perturbations in this sense.

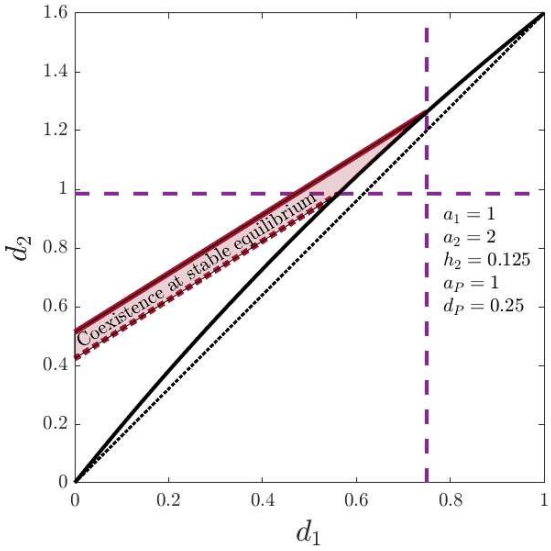

(a) Low handling time

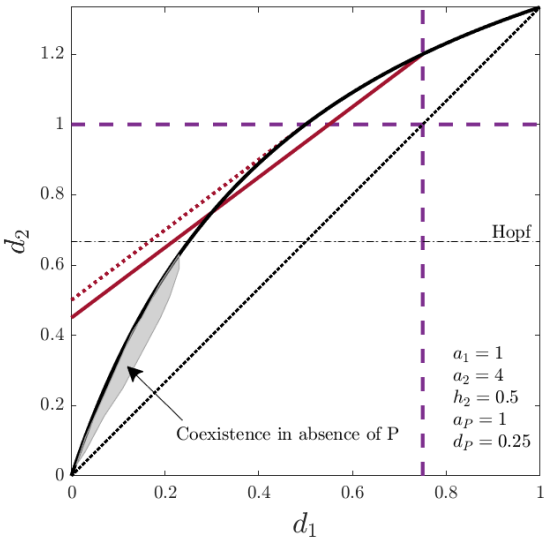

(b) Low attack rate, intermediate handling time

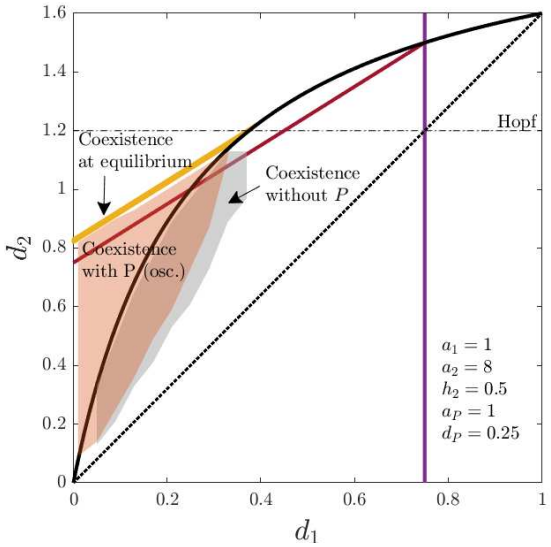

(c) High attack rate, intermediate handling time

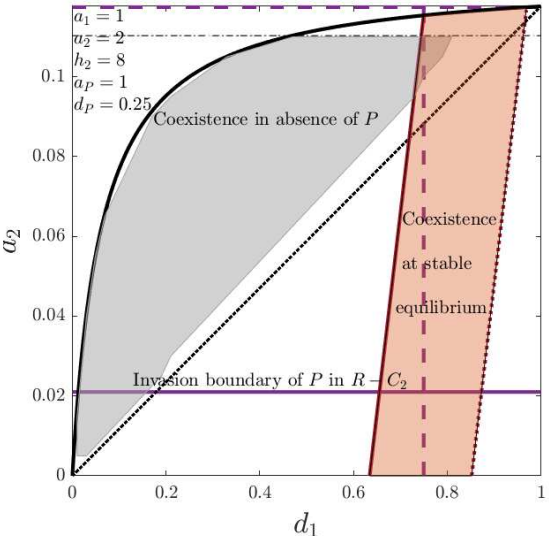

(d) Very high handling time

Figure 3: Effect of attack rate and handling time of the saturating functional response on coexistence in the baseline model (relative nonlinearity and predation) and without predation [old plots]

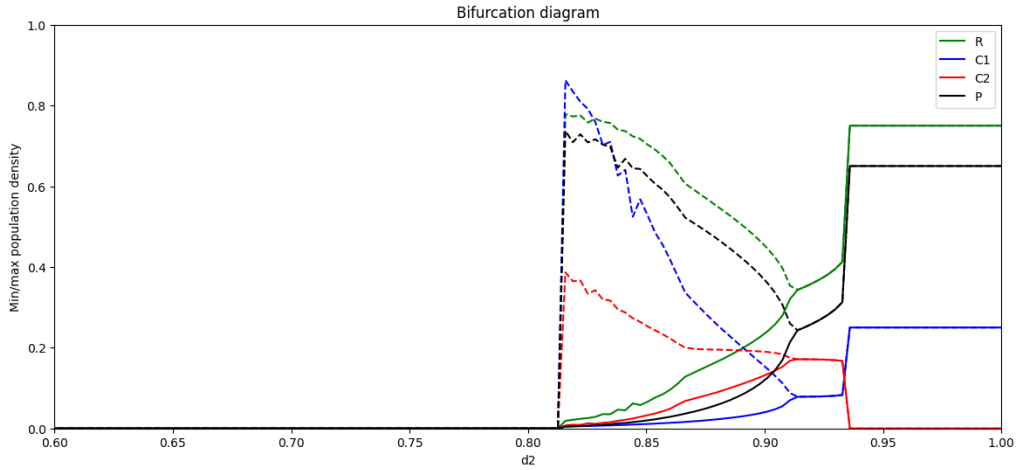

Figure 4: $d_1 = 0.1$, other parameters as in Fig.3c. Initial conditions: with continuation from $d_2 \approx 0.82$ to the right.

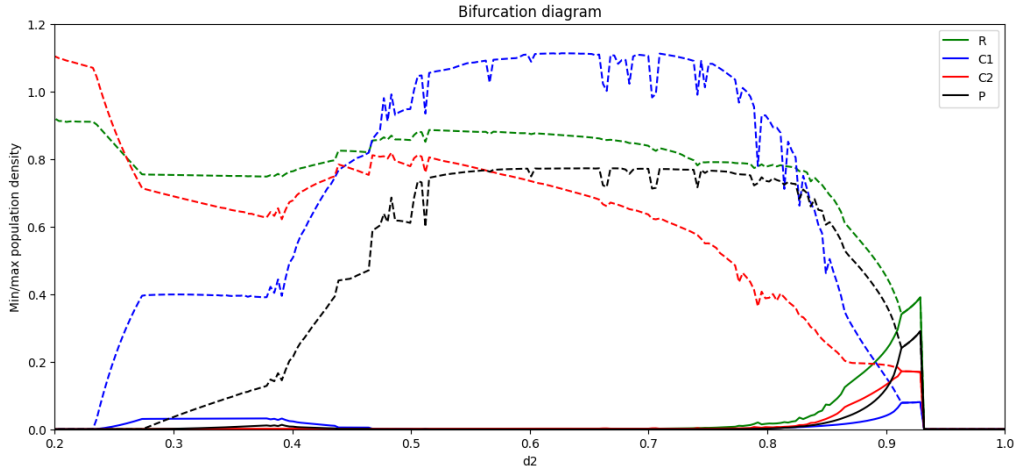

Figure 5: $d_1 = 0.1$, other parameters as in Fig.3c. Initial conditions: with continuation from $d_2 = 0.928$ to the left.

For the third $d_1 - d_2$ plane example (Fig. 3c), we explored the plane with simulations starting from multiple initial conditions. The below images show the coexistence region as found by starting near the E_+ fixed point when it is positive for all species (Fig. 7a) or near the E_- fixed point when it is positive for all species (Fig. 7b). Starting from 0.1 for all species gives a very similar result to the oscillatory area in Fig. 3c but does not show the fixed point equilibrium.

(+ stability of fixed points could be plotted)

- When coexistence is reached from both fixed points, the same attractor is reached (checked for multiple $d_1 - d_2$ values).
- There is bistability between locally stable subsystems, e.g.: $d_1 = 0.3960$ and $d_2 = 1.1881$: $P - C_1 - R$ fixed point or $C_2 - R$ limit cycle; $d_1 = 0.3564$ and $D_2 = 1.1881$: $P - C_1 - R$ fixed point or $P - C_1/C_2 - R$ fixed point; $d_1 = 0.3366$ and $d_2 = 1.1406$: $P - C_1 - R$ fixed point or $C_1/C_2 - R$ limit cycle.

Q: which coexistence areas are relevant? only globally stable seems too restrictive but if the basin of attraction is too small, it is very unlikely to be reached

4.6 Saturating type II functional response for the generalist predator (separate documentation)

Summary:
Qualitatively, the coexistence dynamics produced by the systems are relatively similar to the system with linear predator.

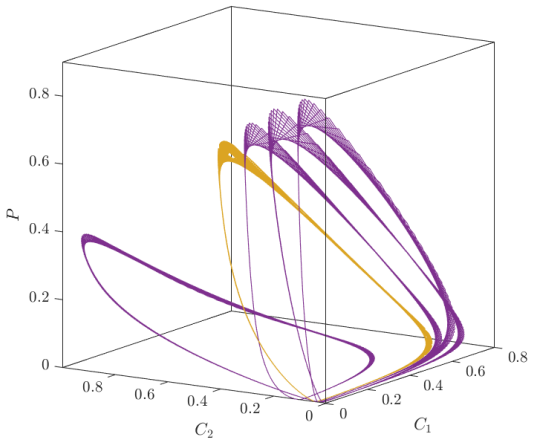

Figure 6: Two locally stable limit cycles resulting from the same model parameters. The curves show the outcome of numerical simulation of the four-species system from two different initial conditions after the convergence period. Parameters: $a_1 = 1$, $a_2 = 8$, $a_P = 1$, $h_2 = 0.4$, $d_1 = 0.02$, $d_2 = 0.2$, $d_P = 0.25$, initial abundance of yellow curve: $[R, C_1, C_2, P] = 10^{-5} \cdot [5.539, 3.962, 0.481, 5.257]$ (perturbation around origin) and of purple curve: e.g. $[0.1, 0.1, 0.1, 0.1]$

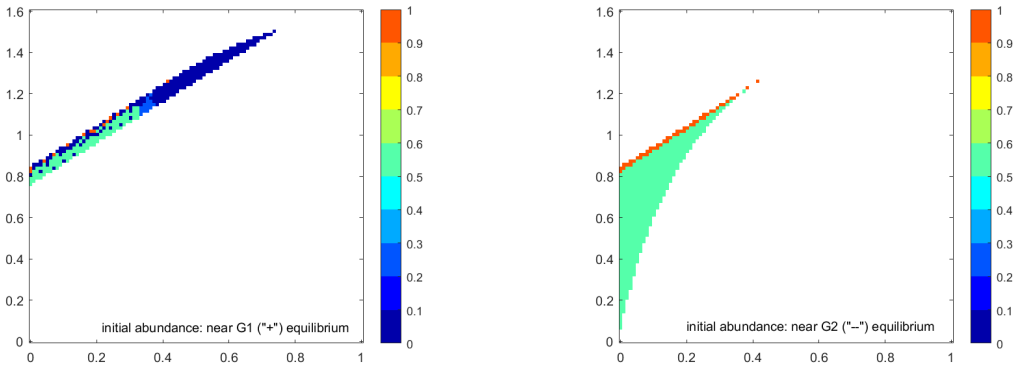

(a) (b)

Figure 7: An example of simulation result starting from different initial conditions for the same model. Dark blue: no coexistence. Orange: coexistence at a stable fixed point. Mint green: coexistence along a cycle.

Quantitatively: depends on the parameter choice for P, longer handling times can be quite destabilizing (in a negative way) but some combinations can lead to relatively large coexistence area when coexistence is impossible with the linear uptake rate.

4.7 Time series analysis

(...)

4.8 Additional mortality rate

When comparing the effects of relative nonlinearity in the $R-C_1/C_2$ model) to the model including predation, the mortality rate experienced by the two consumers will differ by the additional mortality due to predation. We account for this difference to compare the coexistence likelihood between models with similar mortality rates. We approximate the additional mortality that the consumers would experience by the addition of the predator ($a_P P$) from the model with linear consumers and a predator (the predator abundance can be computed analytically). Since the predator abundance depends on the mortality parameters of the consumers, we compute the additional mortality rate for each grid point on the mortality rate plane individually. After adjusting the mortality rates d_1 and d_2 by the additional mortality, we run the same analysis for the model as previously.

Note: we can also do the same for the model with two saturating consumers. However, in this case, the functional responses are not the same as in the case without the additional mortality, since the fitting of the functional response depends on the mortality rate. The model with two saturating consumers and adjusted mortality rate should be comparable to the model with linear and saturating consumers and adjusted mortality rate but not necessarily to the model with two saturating consumers.

(Additional mortality rate implemented but the results seem to be wrong, it needs debugging.)

4.9 Interaction of relative nonlinearity and an emergent growth–defense trade-off

The following figures show the effects of relative nonlinearity, predation and their interaction on the coexistence likelihood.

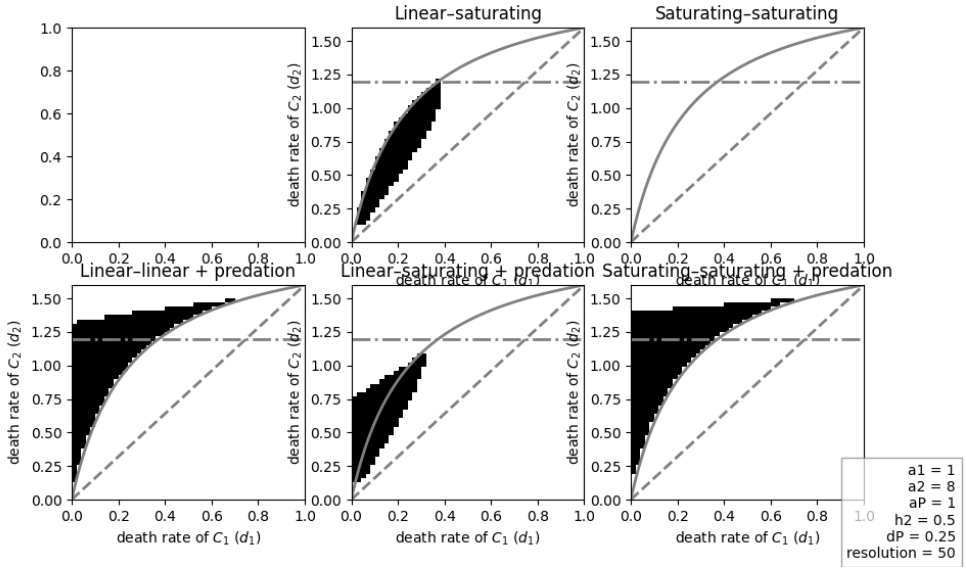

Figure 8: Same parameters as in Fig. 3c.

In the model with predator and two consumers with saturating functional responses, coexistence becomes possible by the presence of the predator. In a larger parameter range, the dynamics show oscillatory behaviour, however, at higher d_2 values, the coexistence is at a stable fixed point.

Lilla: I changed some of the parameters to see how that effects the coexistence areas.

From a similar but different parameter set, change h_2 while keeping all other parameters constant:

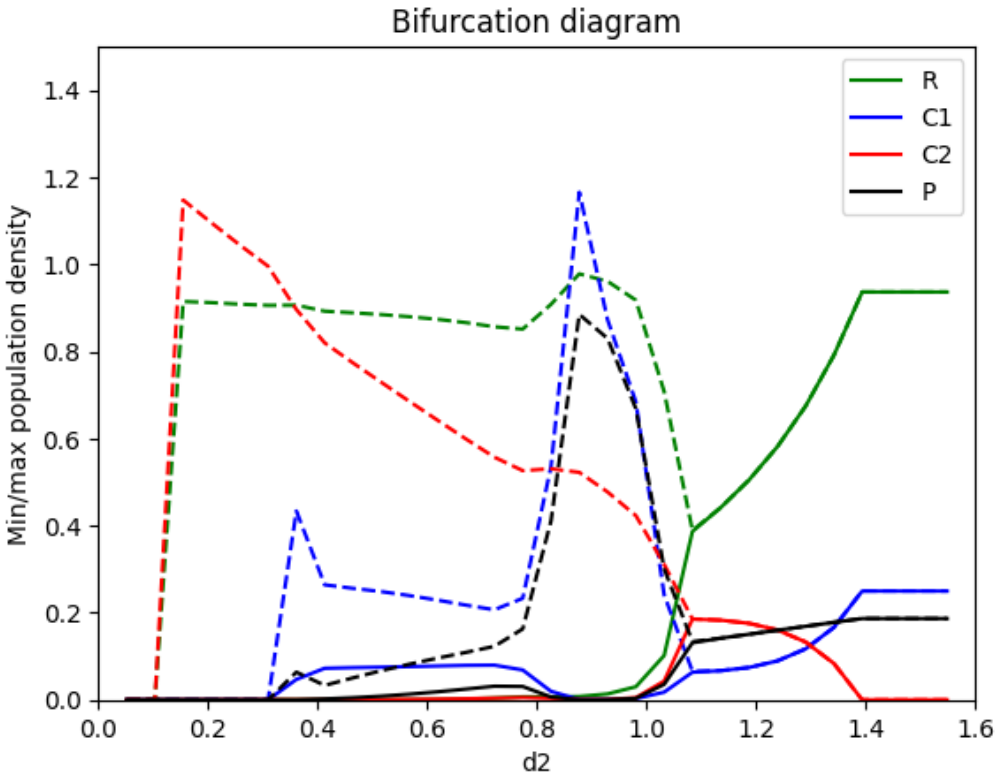

Figure 9: Bifurcation diagram along the d_2 variable in the model with two saturating consumers and a predator. $d_1 = 0.05$, all other parameters as in Fig. 8

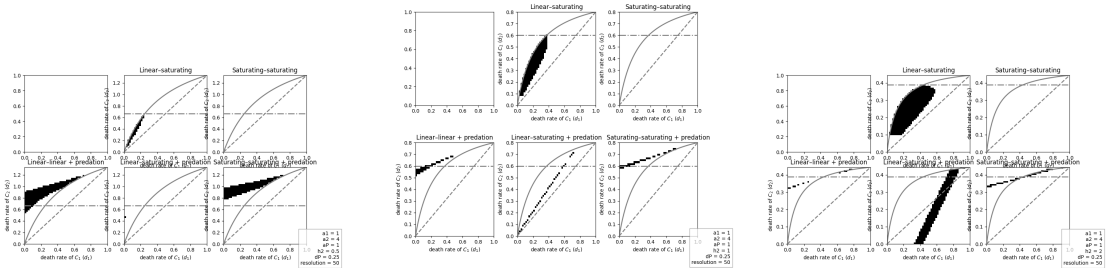

(a) Low h_2 (b) Intermediate h_2 (c) High h_2

Similarly, changing the parameters of the predator. First, a_P (the middle panel will be the same because that is the starting point for altering parameters):

Second, for d_P:

- Perhaps log-changes could make more sense when changing the parameters (although depends on the purpose, we can also just choose one of these that shows the differences between models well)
- Another idea would be to plot the size of the coexistence area with a_2 and h_2 (like the h_2 plots) and then compare for different predator parameters (or we could make an a_P plot in the same manner). It could also be possible to include the type of dynamics in a stacked plot.
- Q: Do the dynamics produced by the satsatpred (both saturating + P) model differ from the linsatpred (baseline with linear, saturating, P) model? Is there a reason we would think the dynamics are not influenced by weak relative nonlinearity? Do the dynamics in the linsat model differ from the linsatpred model?
- FFT for these plots is missing + example time series

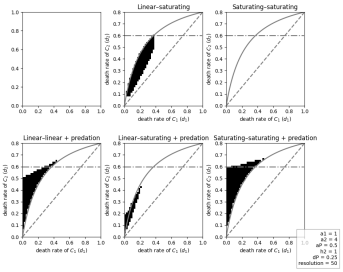

(a) Intermediate h_2, low a_P

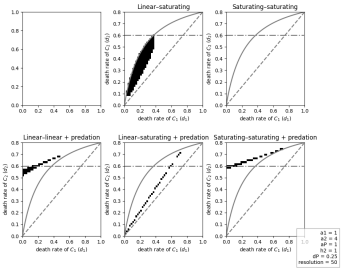

(b) Intermediate h_2, intermediate a_P

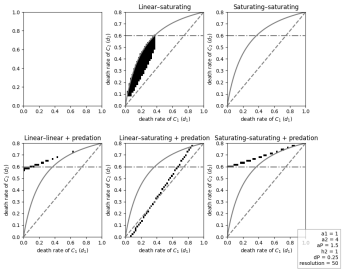

(c) Intermediate h_2, high a_P

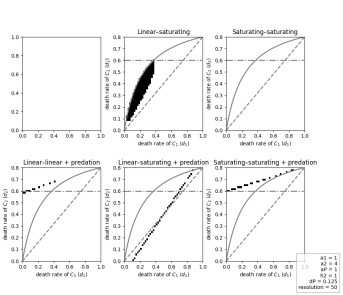

(a) Intermediate h_2, low d_P

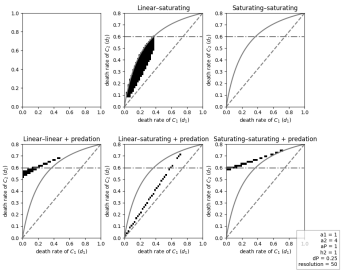

(b) Intermediate h_2, intermediate d_P

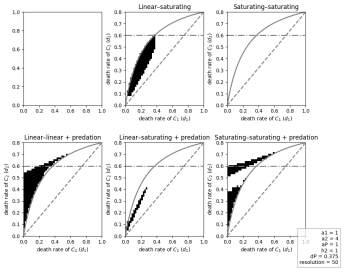

(c) Intermediate h_2, high d_P